



## LA-ICP-MS trace element analysis of magnetite from Gökçedoğan Cu-Zn deposit (Kargı-Çorum) in Central Pontides, Turkey

Cihan Yalçın <sup>1</sup>, Nurullah Hanilçi <sup>2</sup>, Mustafa Kumral <sup>3</sup>, Mustafa Kaya <sup>3</sup>

<sup>1</sup>Ministry of Industry and Technology, General Directorate of Industrial Zones, Ankara, Türkiye, [cihan.yalcin@sanayi.gov.tr](mailto:cihan.yalcin@sanayi.gov.tr)

<sup>2</sup>Istanbul University-Cerrahpaşa, Geological Engineering, İstanbul, Türkiye, [nhanilci@gmail.com](mailto:nhanilci@gmail.com)

<sup>3</sup>Istanbul Technical University, Geological Engineering, İstanbul, Türkiye, [kumral@itu.edu.tr](mailto:kumral@itu.edu.tr); [kayamusta@itu.edu.tr](mailto:kayamusta@itu.edu.tr)

Cite this study: Yalçın, C., Hanilçi, N., Kumral, M., & Kaya, M. (2022). LA-ICP-MS trace element analysis of magnetite from Gökçedoğan Cu-Zn deposit (Kargı-Çorum) in central pontides, Turkey. *Engineering Applications*, 1(1), 11-18

### Keywords

Magnetite  
Formation  
VMS  
Central Pontide  
LA-ICP-MS

### Research Article

Received: 01.04.2022

Revised: 07.05.2022

Accepted: 15.05.2022

Published: 18.06.2022



### Abstract

Magnetite is a common mineral in paragenesis in many mineral deposits, and it is recognized that it covers the conditions of the environment in which it is formed due to its physico-chemical properties. For this reason, chemical compositions of magnetites are used in researches on the origin and formation of ore deposits. Gökçedoğan Cu-Zn massive sulfide deposit (VMS) in the Central Pontides is a syngenetic stratiform deposit observed in metamorphic rocks. The ore paragenesis contains pyrite, chalcopyrite, sphalerite, magnetite, hematite, covellite, malachite, and goethite respectively. Because of its physicochemical properties, in-situ laser-ablation inductively coupled plasma mass-spectrometry (LA-ICP-MS) analysis of magnetite in the ore zone was performed and a new perspective was promoted to the deposit. From analysis Fe is between 72.06-73.39% and O is between 20.78-21.15% respectively. V content is approximately higher than the other trace elements. Analyzes were checked out in both Cu/(Si+Ca)-Al(Zn+Ca) and Cu/Ca-Al(Si+Zn+Ca) diagrams and it was decided that they exhibit similar distributions to VMS deposits in the world. In the spider diagram drew up, it has been showed that Gökçedoğan VMS deposit is close to Besshi Type Windy Craggy deposit with its high Si values.

## 1. Introduction

Magnetite is one of the most common oxide minerals observed in igneous, sedimentary and metamorphic rocks, and it is a mineral that can consist of important signatures in many ore deposits [1-2]. Due to its crystallographic structure, magnetite has an inverted spinel structure where a number of trace elements can replace Fe<sup>2+</sup> or Fe<sup>3+</sup> [3]. Because of its crystallographic structure, magnetite gives important physico-chemical traces of different geological environments [4-7]. It also hides important clues as it preserves the magnetite composition, which has a stable structure due to its physicochemical properties [8]. This mineral is found in paragenesis in many mineral deposits [7, 9]. The physico-chemical conditions in the formation of these mineral deposits still control the composition of the iron oxide minerals. For this reason, magnetites have important data about the formation of the mineral deposit in its paragenesis [10-13]. The geochemical content of magnetite [14], which is generally observed in VMS-type deposits, is used both in the classification and exploration of mineral deposits by in-situ laser-ablation inductively coupled plasma mass-spectrometry (LA-ICP-MS) method [15].

Volcanogenic massive sulfide (VMS) deposits are significant origins for Cu, Zn and Pb, which are formed in many tectonic environments [16]. Volcanogenic massive sulfide (VMS) deposits are separated into 3 major types as Kuroko, Besshi and Cyprus Type [17]. Fox [18] described that pelitic mafic lithologies are relevant for Besshi Type deposits. It is recognized that there are areas similar to the Besshi type deposit, the typical example of which

is in Japan, in various districts around the world. The world's largest Besshi type deposit is the Windy Craggy in northwestern of British Columbia [19]. Magnetite is one of the common minerals in the paragenesis of VMS deposits [20-23] and gets information about the alteration processes, fluid compositions and physicochemical conditions of mineralization [24].

Significant Volcanogenic Massive Sulfide deposits (VMS) are formed along the Pontide orogenic belt, which is one of the main tectonic belts in Turkey. Kuroko or Black Sea type deposits were classified in the Eastern Pontides [25-27] and Cyprus [28] and Besshi type deposits [29-30] in the Central Pontides.

There are rock groups consisting of specific tectonic slices [31] in the Gökçedoğan (Kargı-Çorum) district (Central Pontide). In this district, which is in the subduction-accretionary complex as a tectonic location, units existing to the Kunduz metamorphics mostly crop out [31]. In these metamorphics, Besshi Type Cu-Zn mineralization is observed in parallel with the schistosity within the metabasite and quartzschist alternations [29]. Mainly chalcopyrite, sphalerite, pyrite, magnetite, hematite, covellite, malachite and goethite minerals are observed in ore paragenesis [32]. In this paper, we mention new data gathered from trace element geochemistry of magnetite using LA-ICP-MS.

## 2. Material and Method

In recent years, trace element analyzes of oxide or sulfide minerals have been performed by in-situ laser-ablation inductively coupled plasma mass-spectrometry (LA-ICP-MS) method to point out the genesis of many mineral deposits. With this method, a new perspective has been gained to the mineral deposits [33-36]. Thus, in this study, trace element analysis results of magnetite in the Gökçedoğan Cu-Zn mineralization in the Central Pontides were evaluated.

Electron probe microanalysis studies (EPMA) of magnetite detected in ore paragenesis were carried out in CAMECA SX100 device at ITU ATUM Research and Application Center. Diagrams were set up with the gained data.

### 2.1. Geological Background

In the Central Pontides, lithostratigraphic units of various origin are observed together along the 'suture zones' formed by the closure of the Paleotethys and Neotethys oceans [37-39]. Pre-Jurassic HP/LT metamorphic rock groups and ophiolitic rocks cropping out in extensive areas south of the Central Pontides are the products of a subduction-accretionary complex built up by the closure of the Paleotethys and Neotethys oceans [40-43]. The study area, is located in the Central Pontides, include Middle Jurassic and Cretaceous Accretionary Complex are also named as Central Pontide Supercomplex (Figure 1).

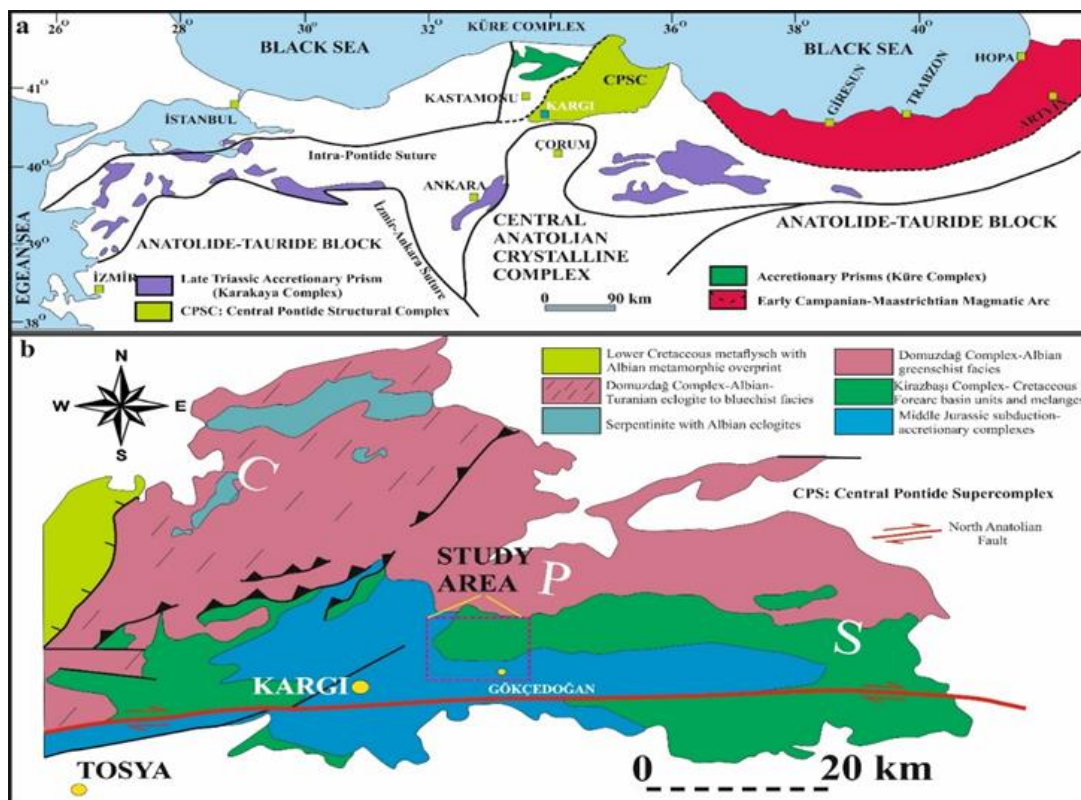


Figure 1. a) Position of the study area between Turkey's structural zones (modified from Günay et al., [30]), b) Position of the study area in the Central Pontide Supercomplex (modified from Aygül et al., [42])

There are rock groups in the Paleozoic-Quaternary age range in this district. The basement of the region consists of the Kunduz metamorphites, which are exhibited of metabasite, gneiss and schists respectively. This unit is overlain by carbonate rocks of Paleozoic-Mesozoic periods with a tectonic contact. In addition, the ophiolitic melange overlies the Kunduz metamorphics in wide areas with thrust faults. With the presence of specific lithostratigraphic sequences, Gökköy, Pelitözü and Ophiolitic mélangé tectonic slices have been described in the region [31].

## 2.2. Mineralization

The stratiform Cu-Zn mineralizations in the study area crop out in the west of Kömürlükdere and Şahin Dere within the Kunduz Metamorphics (Figure 2). Gökçedoğan Cu-Zn mineralization was formed in metabasites belonging to Kunduz metamorphics. Mineralizations are observed in altering levels of metabasite and quartzschist parallel to the schistosity. Along the ore zone, not only chloritization and limonitization are common, but graphitization is also observed at some sequences. In addition, gypsum levels were still observed in the area where Şahin Dere mineralization is located [29]. Mainly actinolite, chlorite, epidote, opaque minerals and quartz are observed in the metabasite with nematoblastic texture (Figure 3).

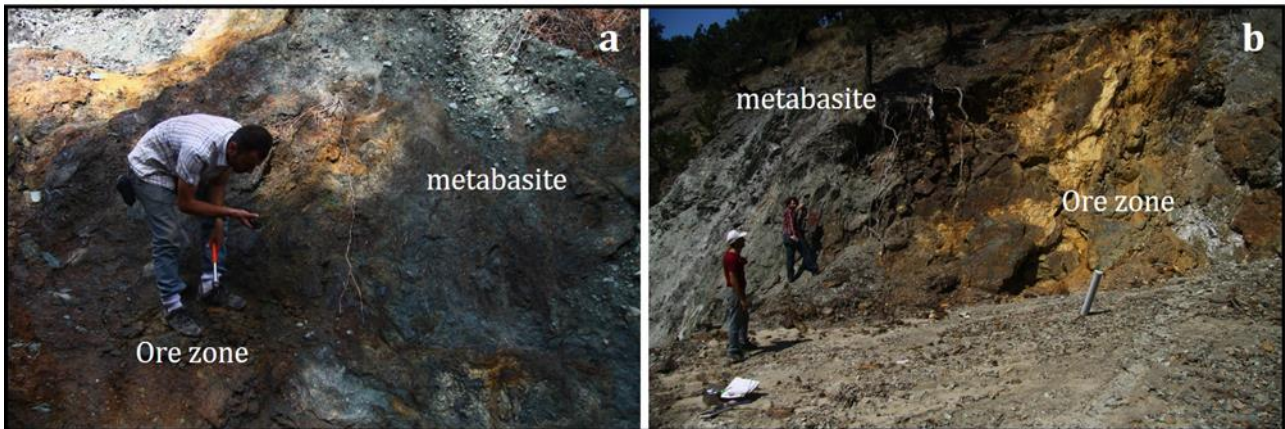


Figure 2. General view of metabasite hosted Cu-Zn mineralization in Gökçedoğan (a. Şahindere, b. Kömürlükdere)

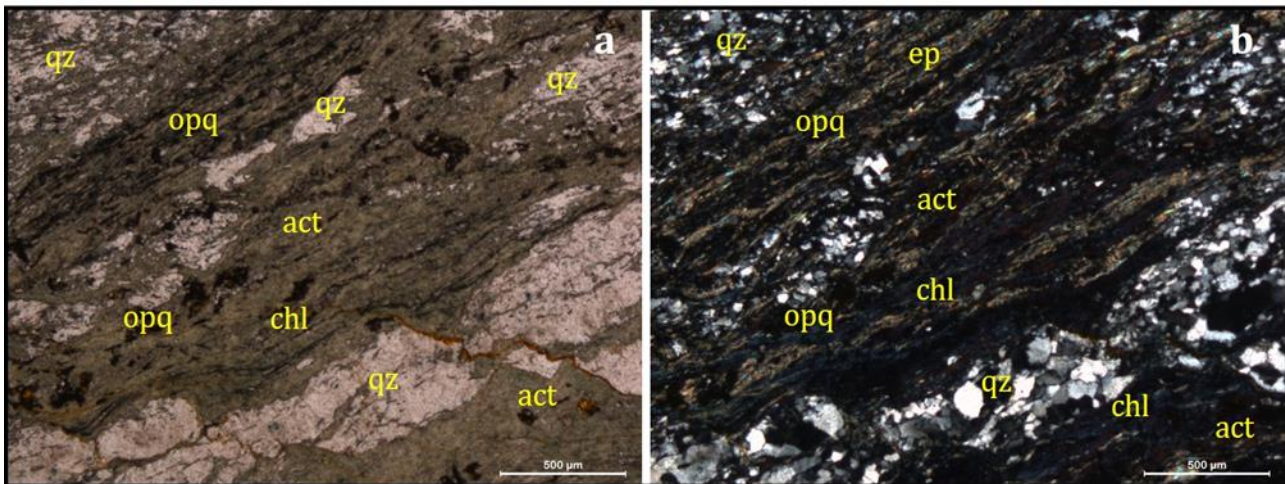


Figure 3. Polarizing microscope images of metabasite, Abbreviations: (act) actinolite, (chl) chlorite, (ep) epidote, (qz) quartz, (opq) opaque mineral

In the ore petrography, it was seen that sphalerites replaced chalcopyrite and pyrite, and pseudocubic magnetites were transformed into hematite [29]. For mineral chemistry, magnetites, which were arranged parallel to the foliation and underwent deformation, were used (Figure 4). In these specimens, magnetites are aligned in one direction owing to the deformation effect (Figure 4a). Although the surface of subhedral and anhedral magnetites is clear and well preserved in general, it has been decided that they are transformed into hematite in places (Figure 4b). On the other hand, hematites are finer grained and generally irregular than magnetites (Figure 4).

Geochemical analyzes of the specimens collected from this district were carried out. Corresponding to the results of the analysis, it was declared that Cu and Zn values in the Kömürlükdere and Göçükdibi ore zones

enriched up to 5 times compared to the clark value [44]. Fe<sub>2</sub>O<sub>3</sub> results are also rather high due to banded pyrite, magnetite, hematite and goethite minerals generally observed in the ore zone.

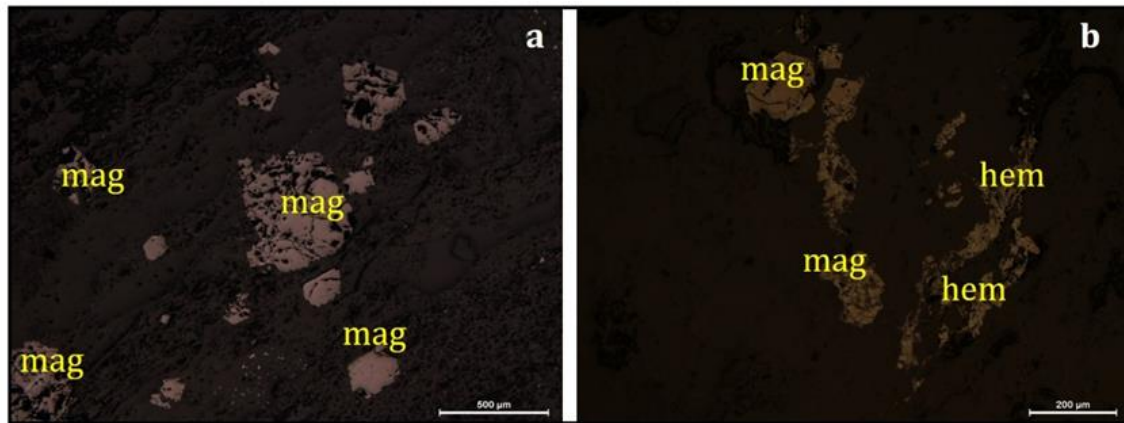


Figure 4. Microscope images of the polished sections. Abbreviations: (mag) magnetite, (hem) hematite

### 3. Results

Mineral chemistry analysis of magnetites in mineral paragenesis was performed to get signatures of the formation of Gökçedoğan Cu-Zn VMS deposit. Since the concentrations of some trace elements in magnetite were below the detection limits, the results of the analysis of only 15 trace elements were obtained. LA-ICP-MS analysis results of magnetite mineral are given in Table 1.

Most trace element abundances in magnetites are less than 0.1 ppm (Table 1). In the samples whose trace element compositions are exceedingly variable, Fe is between 72.06-73.39% and O is between 20.78-21.15% respectively. V is approximately higher than the other elements.

Various diagrams were prepared according to the analysis results obtained. In these diagrams, magnetite analysis results of hydrothermal, skarn, VMS and porphyry deposits are compared.

Gökçedoğan mineralization shows a similar distribution with VMS type deposits on both Al/(Zn+Ca) vs. Cu/(Si+Ca) and Al/(Si+Ca+Zn) vs. Cu/Ca diagrams (Figure 5a, 5b). In the spider diagram, Gökçedoğan mineralization has high Si, identical to the character of the VMS type deposits, and exhibits a distribution similar to the Windy Craggy deposit, which is the largest Besshi Type Deposit (Figure 5c).

Table 1. LA-ICPMS results for trace elements (%) in magnetite from the Gökçedoğan Cu-Zn deposit

%wt	KGD-317	KGD-317	KGD-317	KGD-317	KGD-317
Mg	0,01	0,01	0,01	0,01	0,01
Al	0,02	0,02	0,08	0,01	0,02
Ti	0,02	0,01	0,01	0,01	0,01
V	0,11	0,12	0,06	0,07	0,11
Mn	0,03	0,08	0,02	0,03	0,05
Ni	0,01	0,01	0,03	0,01	0,01
Zn	0,06	0,11	0,28	0,35	0,05
Sn	0,02	0,01	0,02	0,02	0,02
Cr	0,01	0,1	0,1	0,01	0,04
Fe	72,69	73,39	72,07	72,06	72,66
O	20,93	21,15	20,86	20,78	20,92
Cu	0,032	0,045	0,025	0,03	0,03
K	0,002	0,001	0,001	0,002	0,001
Ca	0,055	0,003	0,042	0,031	0,01
Si	0,008	0,6	0,05	0,055	0,013
Total	94,007	95,659	93,658	93,478	93,954

#### 4. Discussion

There is a lack of LA-ICP-MS data for magnetite from VMS deposits in Pontides. For this reason, it is significant to analyze and compare magnetite in VMS deposits according to trace element compositions. In this context, some researchers have previously obtained results with this method.

Singoyi et al. [12] measured the trace element composition of magnetite from VMS deposits in Australia and stated that the Sn/Ga and Al/Co diagram could yield significant results, Nadoll et al. [45] analyzed and evaluated trace elements in magnetite obtained from hydrothermal ore deposits and their host rocks using LA-ICP-MS methods. The same authors still investigated porphyry and skarn Cu deposits in the USA according to the amount of trace elements in magnetites [46]. Makvandi et al. [47] defined three types of magnetite in VMS environments and revealed the geological conditions according to magnetite compositions. These conditions are composition of fluids, temperature, mineralogy, conditions of metamorphism and sources of oxygen and sulfur respectively. In this study, however, the magnetite composition shows that the Gökçedoğan VMS deposit has a character similar to the VMS deposits. In addition, it has been revealed that the Windy Craggy deposit, which is the world's largest Besshi Type VMS deposit, has similarities with magnetite compositions.

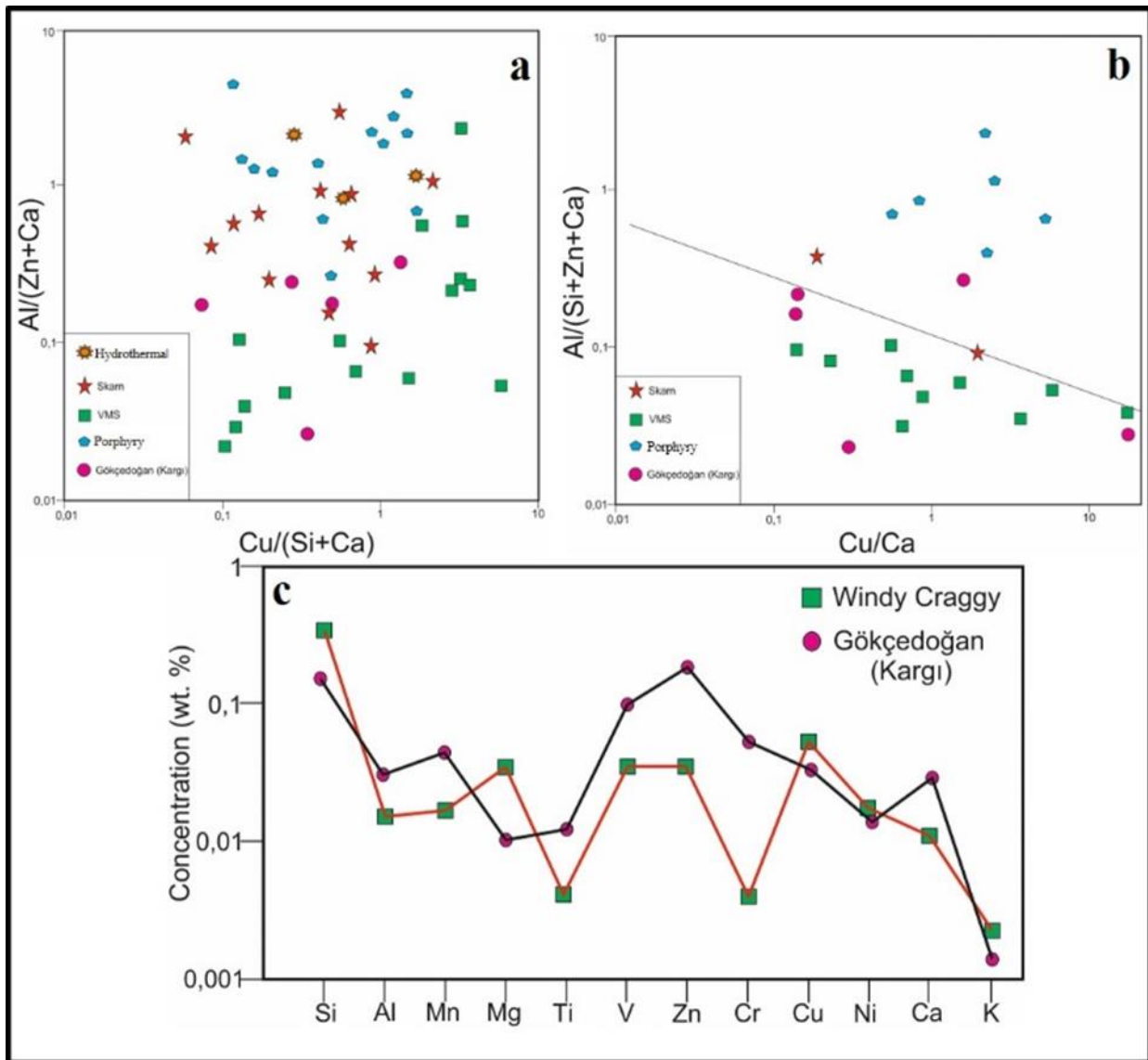


Figure 5. a) Al/(Zn+Ca) vs. Cu/(Si+Ca) diagram, b) Al/(Si+Ca+Zn) vs. Cu/Ca diagram, c) Spider diagram for Besshi Type deposits [48].

#### 5. Conclusion

Gökçedoğan VMS deposit is associated with metabasites in the Central Pontides. The mineralization in the accretionary complex is stratiform type and syngenetic. There are important VMS deposits observed along the Pontide belt, and Cyprus Type and Besshi Type deposits are observed in the Central Pontides. For this reason, it is

important for the metallogenesis of the region to present new approaches with the chemical composition of magnetites in paragenesis in VMS deposits.

Trace element analysis of magnetite in the paragenesis of Gökçedoğan VMS deposit observed in the Central Pontides was carried out. As a result of this study, it was decided that Gökçedoğan Cu-Zn deposit exhibits similar geochemical characteristics with Windy Craggy Besshi Type deposit.

Rapid and efficient results can be obtained by chemical analysis of magnetites in mineral exploration. The results of trace elements of the mineral can be obtained in the analyzes made with the LA-ICP-MS method. As a result of this study, the origin approach of the Gökçedoğan VMS deposit, which is the Besshi type deposit, according to the magnetite composition has been revealed. The number of analyzes should be increased by making measurements from different types of magnetite. Thus, the formation conditions in similar deposits will be comparable.

### **Acknowledgement**

This study is a part of a Ph.D. thesis that was prepared in the Graduate School of Science and Engineering of Istanbul University was supported by TUBITAK project no: 113Y536.

This study was partly presented in 2<sup>nd</sup> Advanced Engineering Days [49] on 16 March 2022.

### **Funding**

This research received no external funding.

### **Author contributions**

**Cihan Yalçın:** Writing-Reviewing and Editing, Geology, Methodology, Geochemistry. **Nurullah Hanılçı:** Ore Geology, Editing, Geochemistry. **Mustafa Kumral:** Ore Petrography, **Mustafa Kaya:** Petrography, EPMA.

### **Conflicts of interest**

The authors declare no conflicts of interest.

### **References**

1. Ramdohr, P. (1980). The ore minerals and their intergrowths. Pergamon, New York.
2. Scheka, S. A., Platkov, A. V., Vezhosek, A. A., Levashov, G. B., & Oktyabrsky, R. A. (1980). The trace element paragenesis of magnetite. Nauka, Moscow, p 147.
3. Nadoll, P., Angerer, T., Mauk, J. L., French, D., & Walshe, J. (2014). The chemistry of hydrothermal magnetite: a review. *Ore Geology Reviews.*, 61, 1–32. <https://doi.org/10.1016/j.oregeorev.2013.12.013>.
4. Lindsley, D. H. (1976). The crystal chemistry and structure of oxideminerals as exemplified by the Fe-Ti oxides. In: Rumble III, D (ed) *Oxide Minerals. Reviews in Mineralogy: Mineralogical Society of America*, pp 1–60.
5. Wechsler, B. A., Lindsley, D. H., & Prewitt, C. T. (1984). Crystal structure and cation distribution in titanomagnetites (Fe<sub>3-x</sub>Ti<sub>x</sub>O<sub>4</sub>). *Am Mineral*, 69, 754–770.
6. Bowles, J. F. W., Howie, R. A., Vaughan, D. J., & Zussman, J. (2011). *Rock-forming minerals- non-silicates: oxides, hydroxides and sulphides*, Second edn. Geological Society, London.
7. Dupuis, C., & Beaudoin, G. (2011). Discriminant diagrams for iron oxide trace element fingerprinting of mineral deposit types. *Miner Depos*, 46, 319–335.
8. Dare, S. A., Barnes, S. J., Beaudoin, G., M'eric, J., Boutroy, E., & Potvin-Doucet, C. (2014). Trace elements in magnetite as petrogenetic indicators. *Mineral. Deposita*, 49 (7), 785–796. <https://doi.org/10.1007/s00126-014-0529-0>.
9. Leach, D. L., Bradley, D. C., Huston, D., Pisarevsky, S. A., Taylor, R. D., & Gardoll, S. J. (2010). Sediment-hosted lead-zinc deposits in Earth history. *Econ. Geol.* 105 (3), 593–625. <https://doi.org/10.2113/gsecongeo.105.3.593>.
10. Carew, M. J. (2004). Controls on Cu-Au mineralization and Fe oxide metasomatism in the Eastern Fold Belt, N.W. Queensland, Australia. Unpublished Ph.D thesis. James Cook University, Queensland
11. Gosselin, P., Beaudoin, G., & Jébrak, M. (2006). Application of the geochemical signature of iron oxides to mineral exploration. GAC-MAC Annual Meeting Prog Abs 31.

12. Singoyi, B., Danyushevsky, L., Davidson, G. J., Large, R., & Zaw, K. (2006). Determination of trace elements in magnetites from hydrothermal deposits using the LA ICP-MS technique. SEG Keystone Conference, Denver, USA.
13. Beaudoin, G., Dupuis, C., Gosselin, P., & Jébrak, M. (2007). Mineral chemistry of iron oxides: application to mineral exploration. In: Andrew CJ (ed) Ninth Biennial SGA meeting. SGA, Dublin, pp 497–500.
14. Xiao, B., Chen, H., Wang, Y., Han, J., Xu, C., & Yang, J. (2018). Chlorite and epidote chemistry of the Yandong Cu deposit, NW China: metallogenic and exploration implications for Paleozoic porphyry Cu systems in the eastern Tianshan. *Ore Geol Rev*, 100:168–182.
15. Lockington, J. A., Cook, N. J., & Ciobanu, C. L. (2014). Trace and minor elements in sphalerite from metamorphosed sulphide deposits. *Miner. Petrol.*, 108 (6), 873–890.
16. Franklin, J. M., Gibson, H. L., Jonasson, I. R., & Galley, A. G. (2005). Volcanogenic Massive Sulphide Deposits. 100th Anniversary Volume. The Economic Geology Publishing Company, pp. 523–560.
17. Pirajno, F., (2009). *Hydrothermal Processes and Mineral System*. Springer, Perth 1–1250.
18. Fox, J. S. (1984). Besshi-type volcanogenic massive sulphide deposits e a review. *Canadian Institute of Mining and Metallurgy Bulletin*, 77, 57e68.
19. Peter, J. M. & Scott, S. D. (1999). Windy Craggy, Northwestern British Columbia: The world's largest Besshi-type deposit – In: Barrie, C. T. & Hannington, M. D. (eds.), *Volcanic-associated massive sulfide deposits. Processes and examples in modern and ancient settings*. *Rev. Econ. Geol.*, 8: 261–295.
20. MacLean, W. H., & Kranidiotis, P. (1987). Immobile elements as monitors of mass transfer in hydrothermal alteration; Phelps dodge massive sulfide deposit Matagami, Quebec. *Econ Geol*, 82:951–962.
21. Sillitoe, R. H. (2010). Porphyry copper systems. *Econ Geol*, 105:3–41.
22. Zhong, R. C., Li, W. B., Chen, Y. J., & Huo, H. L. (2012). Ore-forming conditions and genesis of the Huogeqi Cu–Pb–Zn–Fe deposit in the northern margin of the North China Craton: evidence from ore petrologic characteristics. *Ore Geology Reviews*, 44, 107–120.
23. Zhou, Z., Tang, H., Chen, Y. C. Z. (2017). Trace elements of magnetite and iron isotopes of the Zankan iron deposit, westernmost Kunlun, China: a case study of seafloor hydrothermal iron deposits. *Ore Geol Rev* 80: 1191–1205.
24. Bryndzia L. T., & Scott, S. D. (1987). The composition of chlorite as a function of sulfur and oxygen fugacity; an experimental study. *Am J Sci*, 287: 50–76.
25. Çiftci, E., & Hagni, R. D. (2005). Mineralogy of the Lahanos deposit a Kuroko-type volcanogenic massive sulfide deposit from the eastern Pontides (Giresun, NE Turkey). *Geol. Bull. Turk.*, 48 (1), 55–64.
26. Eyüboğlu, Y., Santosh, M., Keewook, Y., Tüysüz, N., & Korkmaz, S. (2014). The Eastern Black Sea-type volcanogenic massive sulfide deposits: geochemistry, zircon U-Pb geochronology and an overview of the geodynamics of ore genesis. *Ore Geology Reviews*, 59, 29–54.
27. Revan, M. K., Genc, Y., Maslennikov, V. V., Maslennikova, S. P., Large, R. R., & Danyushevsky, L. V. (2014). Mineralogy and trace-element geochemistry of sulfide minerals in hydrothermal chimneys from the Upper-Cretaceous VMS deposits of the Eastern Pontide orogenic belt (NE Turkey). *Ore Geology Reviews*, 63, 129–149.
28. Ustaomer, T., & Robertson, A. H. F., (1994). Late Palaeozoic marginal basin and subduction accretion: the Palaeotethyan Kure Complex, Central Pontides, northern Turkey. *J. Geo. Soc London*, 151, 291–305.
29. Yalçın, C. (2018). *Geology and formation of the Gökçedoğan (Kargı-Çorum) Cu ± Zn mineralization*. PhD Thesis, İstanbul University, Institute of Graduate Studies in Science and Engineering, 301.
30. Günay, K., Dönmez, C., Oyan, V., Yıldırım, N., & Çiftçi, E. (2018). Geology and geochemistry of sediment-hosted hanönü massive sulfide deposit (Kastamonu – Turkey). *Ore Geology Reviews*, 101, 652–674.
31. Yalçın, C., Haniçlı, N., Kumral, M., & Kaya, M. (2022). Formation and Tectonic Evolution of Structural Slices in Eastern Kargı Massif (Çorum, Turkey). *Bulletin of the Mineral Research and Exploration*. Doi: 10.19111/bulletinofmre.1067604.
32. Yalçın, C., Haniçlı, N., Kumral, M., & Kaya, M. (2022). Magnetite Geochemistry of Beshhi-type Cu-Zn Mineralizations in Central Pontides (Kargı-Çorum). *2nd Advanced Engineering Days*, 30–32.
33. Mukherjee, I. & Large, R. (2017). Application of pyrite trace element chemistry to exploration for SEDEX style Zn-Pb deposits: McArthur Basin, Northern Territory, Australia. *Ore Geology Reviews*. 81, 1249–1270.
34. Hu, X., Chen, H.Y., Zhao, L.D., Han, J.S. & Xia, X.P. (2017). Magnetite geochemistry of the Longqiao and Tieshan Fe–(Cu) deposits in the Middle-Lower Yangtze River Belt: Implications for deposit type and ore genesis. *Ore Geology Reviews*, 89, 822–835.
35. Kampmann, T. C., Jansson, N. F., Stephens, M. B., Olin, P. H., Gilbert, S. & Wanhainen, C. (2018). Syn-tectonic sulphide remobilization and trace element redistribution at the Falun pyritic Zn-Pb-Cu-(Au-Ag) sulphide deposit, Bergslagen, Sweden. *Ore Geology Reviews*, 96, 48–71.
36. Li, D. F., Fu, Y., Sun, X. M., Hollings, P., Liao, J. L., Liu, Q. F., Feng, Y. Z., Liu, Y. & Lai, C. (2018). LA-ICP-MS trace element mapping: Element mobility of hydrothermal magnetite from the giant Beiya Fe-Au skarn deposit, SW China. *Ore Geology Reviews*, 92, 463–474.
37. Robertson, A. H. F. (2002). Overview of the genesis and emplacement of Mesozoic ophiolites in the Eastern Mediterranean Tethyan Region. *Lithos*, 65, 1–67.

38. Robertson, A. H. & Ustaömer, T. (2004). Tectonic evolution of the Intra-Pontide suture zone in the Armutlu Peninsula, Nw Turkey. *Tectonophysics*, 381, 175–209.
39. Okay, A. I., Tüysüz, O., Satır, M., Özkan-Altner, S. & Altner, D. et al. (2006). Cretaceous and Triassic subduction-accretion, HP/ LT metamorphism and continental growth in the Central Pontides, Turkey. *Geological Society of America Bulletin*, 118, 1247–1269.
40. Okay, A. I., Gürsel, S., Sherlock, S., Altner, D. & Tüysüz, O. et al. (2013). Early Cretaceous sedimentation and orogeny on the active margin of Eurasia: Southern Central Pontides, Turkey. *Tectonics*, 32, 1247–1271.
41. Aygül, M., Okay, A. I., Oberhänsli, R., Schmidt, A. & Sudo, M. (2015). Late Cretaceous infant intra-oceanic arc volcanism, the Central Pontides, Turkey: petrogenetic and tectonic implications. *Asian Journal of Earth Science*. <https://doi.org/10.1016/j.jseaes.2015.07.005>.
42. Aygül, M., Okay, A. I., Oberhänsli, R. & Sudo, M. (2016). Pre-collisional accretionary growth of the southern Laurusian active margin, Central Pontides, Turkey. *Tectonophysics*, 671, 218–234.
43. Çelik, Ö. F., Chiaradia, M., Marzoli, A., Özkan, M. & Billor, Z. et al. (2016). Jurassic metabasic rocks in the Kızılırmak accretionary complex (Kargı region, Central Pontides, Northern Turkey). *Tectonophysics*, 672–673, 34–49.
44. Yalçın, C., Hanilçı, N., Kumral, M. & Kaya, M. (2018), Geochemistry of Kömürlükdere and Göçükdibi (Kargı-Çorum) Cu-Zn Mineralization, VIII. Geochemistry Symposium, Abstract books, p. 138-139, 02-06 May, Manavgat, Antalya, Turkey.
45. Nadoll, P., Mauk, J. L., Hayes, T. S., Koenig, A. E. & Box, S. E. (2012). Geochemistry of magnetite from hydrothermal ore deposits and host rocks of the Mesoproterozoic Belt Supergroup, United States. *Econ. Geol.* 107, 1275–1292.
46. Nadoll, P., Mauk, J. L., Leveille, R. A. & Koenig, A. E. (2015). Geochemistry of magnetite from porphyry Cu and skarn deposits in the southwestern United States. *Miner. Depos.* 50, 493–515.
47. Makvandi, S., Ghasemzadeh-Barvarz, M., Beaudoin, G., Grunsky, E. C., McClenaghan, M. B., Duchesne, C. & Boutroy, E. (2016). Partial least squares-discriminant analysis of trace element compositions of magnetite from various VMS deposit subtypes: Application to mineral exploration. *Ore Geol. Rev.* 78, 388–408. <https://doi.org/10.1016/j.oregeorev.2016.04.014>.
48. Beaudoin, G. & Dupuis, C. (2009). Iron-oxide trace element fingerprinting of mineral deposit types. In: Mumin, H., Corriveau, L. (Eds.), *Exploring for Iron Oxide Copper-Gold Deposits: Canada and Global Analogues*, Short Course, Geological Association of Canada Annual Meeting, Québec City, 107–121.
49. Yalçın, C., Hanilçı, N., Kumral, M., & Kaya, M. (2022). Magnetite geochemistry of Beshhi-type Cu-Zn mineralizations in Central Pontides (Kargı-Çorum). *Advanced Engineering Days (AED)*, 2, 30-32.



© Author(s) 2022. This work is distributed under <https://creativecommons.org/licenses/by-sa/4.0/>